

# Production of Super Heavy Elements at GANIL: present status and perspectives

S. Grévy<sup>a</sup> and FULIS collaboration:

N. Alamanos<sup>b</sup>, N. Amar<sup>a</sup>, J.C. Angélique<sup>a</sup>, R. Anne<sup>c</sup>,  
G. Auger<sup>c</sup>, F. Becker<sup>c</sup>, R. Dayras<sup>b</sup>, A. Drouart<sup>b</sup>,  
J.M. Fontbonne<sup>a</sup>, A. Gillibert<sup>b</sup>, D. Guerreau<sup>c</sup>, F. Hannape<sup>a</sup>,  
R. Hue<sup>c</sup>, A.S. Lalleman<sup>c</sup>, T. Legou<sup>a</sup>, R. Lichtenthäler<sup>d</sup>,  
E. Liénard<sup>a</sup>, W. Mittig<sup>b</sup>, F. De Oliveira<sup>b</sup>, N. Orr<sup>a</sup>,  
G. Politi<sup>e</sup>, Z. Sosin<sup>f</sup>, M.G. Saint-Laurent<sup>c</sup>,  
J.C. Steckmeyer<sup>a</sup>, C. Stodel<sup>c</sup>, J. Tillier<sup>a</sup>, R. de Turreil<sup>c</sup>,  
A.C.C. Villari<sup>c</sup>, J.P. Wieleczko<sup>c</sup> and A. Wieloch<sup>f</sup>.

<sup>a</sup>LPC, IN2P3-ISMRA-Université, Caen, F-14050, France

<sup>b</sup>DAPNIA/SPhN, CEA Saclay, Gif-sur-Yvette, France

<sup>c</sup>GANIL, Caen, France

<sup>d</sup>IFUSP, São Paulo, Brazil

<sup>e</sup>Università di Catania, Italy

<sup>f</sup>Ins. Fizyki Uniw., Krakow, Poland

proceeding to the ASR2001 Conference, to be published  
in the Journal of Nuclear and Radiochemical Sciences (june 2002)

## Abstract

Experiments on the production and study of superheavy nuclei have been undertaken at GANIL taking advantages of the powerful velocity filter LISE3 and the high intensity ECR ion sources. A complete set-up has been built: - reaction chamber containing large rotating wheels, - slits and beam profiler at mid-filter, - detection chamber with time-of-flight and Silicon detectors for identifying evaporation residues and their decay products. The response was checked via fusion reactions with known cross sections producing known  $\alpha$ -decay chains and fission fragments. Excellent transmission of evaporation residues and rejection factor for the primary beam were obtained. This device is presented together with the results obtained in our last experiments and our future plans are discussed.

# 1 Introduction

An experimental program dedicated to the study of Super Heavy Elements (SHE) started at GANIL in order to take advantages of the performances of the accelerator and of the powerful velocity filter LISE3.

Indeed because of the very low cross sections for the production of SHE (from 1  $\mu$ barn for  $Z=100$  to 1 pbarn for  $Z=112$ ) [1], very high intensity ECR ion sources delivering about one particle- $\mu$ A ( $6.27 \times 10^{12}$  projectiles/sec) or more should be used. The second important point is the separation between the projectiles and the complete fusion evaporation residues (ER) emitted at forward angle after the production target. Originally, the LISE3 Wien filter [2] was designed to improve the separation of exotic nuclei produced by fragmentation of the projectile and selected by the LISE spectrometer. Then, an important work has been done to adapt it to fusion experiments improving its ability to work with very high primary beam intensities.

An experimental setup composed of a dedicated rotating target, beam diagnostics, time detectors and a set of Si-detectors (for the implantation and decay products) has been developed. Finally a digital electronics is under development to reach extremely short decay times in the order of few  $\mu$ -seconds.

The response of the whole setup was checked via fusion reactions with known cross sections and  $\alpha$  decay chains:  $^{204,206}\text{Fr}_{87}$  nuclei formed via  $^{86}\text{Kr} + ^{\text{nat}}\text{Sb}$  with cross sections of 10 to 300  $\mu$ barn [4]. These equipments were then used for an experiment dedicated to the system  $^{86}\text{Kr}$  on  $^{208}\text{Pb}$  and the transmission and the rejection factor of the Wien filter were precisely measured in an experiment dedicated to the production of the Sg element ( $Z=106$ ) through the system  $^{54}\text{Cr} + ^{208}\text{Pb}$ . Comparison with known values for the excitation energy function [1] allowed to check the excellent transmission together with an high rejection factor.

An experimental program has been established for the production of new elements and/or new isotopes with two principal axes: – *i*– the use of the inverse kinematics with a beam of Lead and – *ii*– the use of the neutron-rich  $^{76}\text{Ge}$  as projectile. Another program dedicated to the study of the properties of SHE has also started recently.

## 2 Experimental setup

A general overview of the experimental setup, from the reaction chamber to the detection setup is presented in Figure 1.

### 2.1 Reaction chamber

The reaction chamber contains two 67 cm diameter wheels bearing 35 targets ( $5.0 \times 1.5$  cm<sup>2</sup> each) and rotating up to 2000 RPM, allowing targets with low melting temperature (like Pb or Bi) to sustain very intense primary beams. The second wheel support carbon stripper foils in order to re-equilibrate the charge state of evaporation residues. The time structure of the beam is synchronized with the rotation. Two smaller wheels allow us to run with targets having higher melting temperatures. A Si detector continuously monitors the status of each target via elastic scattering reactions.

## 2.2 Wien filter

The LISE3 Wien filter has crossed magnetic and electric fields in a rather compact geometry and its angular acceptance is  $\pm 36\pi$  mrad. It is divided into two identical halves and is followed by a dipole magnet. Several modifications were found to be necessary for fusion experiments: *-i-* the upper plate in the first half of the filter was moved up by 2 cm in order to deflect the beam without hitting the electrode. The beam is now stopped on a new water-cooled collimator, *-ii-* two pairs of independently movable slits and a beam profiler were installed at mid-filter. An additional background suppression can be performed using the last dipole magnet located between the Wien filter and the detection chamber. The transmission of fusion nuclei from the target position through the quadrupoles, filter and final dipole was studied via a simulation code [3]. The optics are checked and the Wien filter is calibrated using low energy ions (0.35 MeV/u to have the same speed than ER's after the target).

## 2.3 Detectors

The detection setup (see Figure 2) is composed of two Galottes (carbon foils + MCP's time detectors) and 13 Si detectors. The time detectors are used in order to tag all the events (ER's or background) coming from the beam. Since the efficiency of Galotte for light particles might not be 100%, two of them are used. Then, the "implantation events" are those with an implantation energy signal in coincidence with both Galottes whereas the " $\alpha$ " or fission events are those in anti-coincidence. The implantation detector is a  $300\mu\text{m}$  thick Si 48x48 strips. The distance between the strips is reduced ( $\sim 45\mu\text{m}$ ) to have a dead zone inferior to 5%. Two of them are mounted on a movable arm. When emission of  $\alpha$ -particles or fission fragments is identified via electronics, the beam is immediately stopped for a short while during which the first implantation detector is moved out of the beam and the second implantation detector comes in, then the beam is sent again. This technique allows us to wait for very long decay times in the first implantation detector, being completely free of background coming from the beam. The ER's are implanted at a depth of approximately  $10\mu\text{m}$  which is smaller than the range in Si for  $\alpha$  particles with energy above 2.5 MeV. Then, in order to measure the full energy of the  $\alpha$  particles emitted at backward angles which escape the implantation detector, a set of 8 Si detectors is mounted in a 'tunnel' geometry. With this configuration, the efficiency for full  $\alpha$  energy goes up from 55 to 95%. A 'face' Si detector is placed in front of the 'out of beam' implantation detector in order to play the same role, the efficiency being then 100%. A veto Si detector is placed after the implantation detector to eliminate the background of light particles coming from the beam. All the Si detectors are mounted on copper supports and can be cooled to reduce the electronic noise.

## 2.4 Data acquisition and Electronics

Specific electronics and data acquisition systems were developed. We use for the data acquisition a complete VXI system for which the standard dead-time is around  $150\mu\text{s}$ . In order to reduce it, a multi-trigger logic with 2 sets of converters (ADC's) is working in the following way: the hard trigger provided by the electronics enters into two GMT (Ganil Master Trigger) modules, T1 and T2. In case of usual counting

rate, all the triggers are treated as 'T1' and the events are registered into the first set of converters. This way is exactly the same as the usual one used in many experiments. The same signals are also duplicated into the second set of converters but are not yet considered by the acquisition. In case of a new trigger comes during the dead time of GMT1, it is now treated by GMT2 (as a trigger 'T2') while GMT1 continues to deal with the preceding event. The minimum time between two events is then about  $30\mu s$ . This procedure was tested with a strong  $\alpha$ -source before the experiment. The used converters are new 14-bits ADC's which allow to have a good resolution for  $\alpha$ -particles (less than 50 keV) together with a large range of energy, between 300 keV and 250 MeV (necessary for spontaneous fission events).

A fast analysis program allows us to identify 'on line'  $\alpha$ -decay chains or spontaneous fission and then to stop the beam and move out the implantation detector (see sect. 2.3)

A complete read out digital electronics is actually under development to be able to reach extremely short decay times, in the order of few  $\mu sec$  keeping good energy resolution (less than 50 keV) on a large energy range from 1 MeV to 1 GeV. This new digital electronics will be placed after the analog front-end electronics (preamplifiers) and the main idea of such an approach is to adapt a dedicated processing to each event on a very large dynamical range and without limitation due to the recovery time of the preamplifier.

## 3 Experimental results

### 3.1 Experiment on $^{86}\text{Kr} + ^{208}\text{Pb}$ system

In July 1999, the BGS-Berkeley group reported the observation of 3 events of the new element  $Z=118$  identified by  $\alpha$ -decay with chains of 6  $\alpha$ 's [5]. The reported cross section was much larger than expected ( $\sim 2$  pb) and the same system studied with the velocity filter SHIP at Darmstadt did not lead to the observation of this element [7], justifying to repeat this experiment at GANIL in december 99. Since GANIL is able to deliver an high intensity beam of  $^{86}\text{Kr}$  ( $15\mu A$  with charge  $10+$ , i.e. nearly  $10^{13}$  projectiles/sec), our idea was to confirm (or not) Berkeley's result and, in the case of a positive answer, to obtain additional information: *-i-* be able to reach shorter decay times (by the use of fast electronics, see sect. 2.4.) for possible  $\alpha$  decay before the minimum time of 120  $\mu sec$  in the Berkeley experiment, *-ii-* wait for very long decay times (by the use of movable implantation detectors, see sect. 2.3.), *-iii-* since ER's may be created in an isomeric state which decays via electron capture followed by an electron cascade with an unknown half-live modifying the ionic charge and strongly reducing the transmission in the case of the GSI experiment, the carbon stripper foils were in our experiment located at a distance from the target 3 times larger than in the SHIP experiment.

With a total accumulated dose of  $1.1 \times 10^{18}$  ions at 5.27 MeV/u on targets of  $300 \mu g/cm^2$ , we didn't observe any event corresponding to the decay of element 118.

The result of Berkeley was recently retracted [6].

### 3.2 Experiment on $^{54}\text{Cr} + ^{208}\text{Pb}$ system

In order to measure precisely the transmission and the rejection factor of the LISE3 Wien filter for SHE's, an experiment dedicated to the production of the  $\text{Sg}_{106}$  el-

ement through the system  $^{54}\text{Cr}$  on  $^{208}\text{Pb}$  was performed at GANIL in december 2000. With a primary beam intensity of 40 nAp and 2 incident energies (4.698 and 4.756 MeV/u), we observed 10 events of  $^{261}\text{Sg}_{106}$  (1 neutron evaporation channel) and 2 events of  $^{260}\text{Sg}_{106}$  (2 neutrons evaporation channel). The decay chains were identified by position correlation between the implantation of the ER and the decay events in the implantation detector. Comparison with the known excitation energy functions [1] makes possible to deduce a transmission efficiency above 60% together with a power of suppression of the primary beam and scattered projectiles of  $\sim 2 \times 10^{10}$ , corresponding to a counting rate of 5-10 Hz in the implantation detector.

## 4 Short and Middle range Perspectives

### 4.1 Inverse kinematics

#### 4.1.1 Method

The use of the inverse kinematics (heavy projectile on light target) has been tried at GANIL in June 1999 and will be used in spring 2002 on the system  $^{208}\text{Pb} + ^{54}\text{Cr}$  to produce  $^{261,260}\text{Sg}_{106}$  isotopes [8]. This technique presents several assets in comparison with direct kinematics

- i- the target thickness is no longer limited by multiple scattering of the ER's and it becomes possible to use thicker targets covering an excitation energy range of typically 10 MeV instead of 3-4 MeV. The counting rate is then maximized and the gain in time can be very important. Indeed, in the search for new isotopes or new elements, the incident energy depends strongly on the mass defects which differ in different mass tables by several MeV whereas the excitation function is rather narrow.

- ii- the ER's are more strongly focussed at forward angles resulting in a better transmission through the LISE3 filter.

- iii- because of the higher energy after the target, the ionic charge distribution of ER's is better estimated and its relative width is smaller. Here again the transmission is favoured.

- iv- finally, the quality of the data is better: due to the deeper implantation depth, the energy deposited by the ER's is higher, both fission fragments are stopped and escaping  $\alpha$  particles lose more than 2 MeV and then cannot be missed.

The main drawback of this approach concern the velocity difference between the beam and the ER's which is much smaller than in direct kinematics. Then, higher electric and magnetic fields are necessary in the Wien filter. With the new power supplies installed this year, the LISE3 filter will be able to get the same spatial separation at mid-filter as in direct kinematics.

#### 4.1.2 Use of $^{208}\text{Pb}$ beam

Several systems can be studied for different purposes (summarized in Table 1):

- i- *New paths to known isotopes with  $^{208}\text{Pb}$* : Produce the same isotopes of the odd Z compound nuclei than ER's formed at GSI with a  $^{209}\text{Bi}$  target [1]. Here, two points are of interest: first, measure and then compare the cross sections which will give a clue to the respective roles of macroscopic and structure effects: charge

asymmetry of the entrance channel and closed shells effects. Secondly, produce ER's in different levels, especially isomeric states.

–ii – *New isotopes with  $^{207}\text{Pb}$*  : Produce isotopes lighter by 1 neutron than the ones known for several elements:  $^{260}\text{Bh}_{107}$ ,  $^{265}\text{Mt}_{109}$ ,  $^{271}\text{111}$  and  $^{276}\text{112}$ . For the last two cases, a chain of 3  $\alpha$ 's will be observed before reaching a known isotope, i.e. 3 new isotopes will be observed in one event.

–iii – *New elements* : Above  $Z=109$  the counting rates are very low. For  $^{277}\text{112}$ , measurements were made at one beam energy only, not necessarily at the maximum of the excitation function. The broader energy coverage provided by inverse kinematics may reveal a larger cross section. Moreover, the 1n channel cross section decreasing quickly with  $Z$ , it may be that the 0n cross section becomes larger even through the fusion probability drops very much at the corresponding incident energy. Added to the uncertainty on the compound nucleus mass defect, the exploration of a broad range of incident energies corresponding to 0n+1n channels leads to lengthy measurements at several incident energy in direct kinematics: 6 beam energies were tried for Se+Pb at GSI in the search of element 116 [1] whereas an excitation energy range of 12 MeV or more can be covered with a single incident energy in inverse kinematics.

## 4.2 Use of $^{76}\text{Ge}_{32}$ beam

The main interest of using  $^{76}\text{Ge}$  beam is the **direct** cold fusion production of the element  $^{273}\text{110}$  using a  $^{198}\text{Pt}$  target [9]. Indeed, this isotope has been observed in 3 events only through the decay of element  $^{277}\text{112}$  and possibly 3 events by direct production in **hot** fusion reaction ( $^{34}\text{S}+^{244}\text{Pu}=\text{}^{273}\text{110}+5\text{n}$ ). A very large range of  $\alpha$ -decay energies, from 9.18 to 11.17 MeV with lifetimes from 0.11 to 170 msec have been observed. What we propose is to make a precise  $\alpha$ -spectroscopy of this isotope since the population of different levels (especially isomeric states) may be due to overreaching the deformed shell  $N=162$ . This would require a "large" number of events.

A more general interest for the  $^{76}\text{Ge}$  beam is provided by the accessible region of production. Indeed, it makes possible, using targets ranging from  $^{192}\text{Os}_{76}$  to  $^{205}\text{Tl}_{81}$ , to produce elements 108 to 113 heavier by two neutrons (except for element 111) than the isotopes produced using Pb/Bi targets with beams ranging from  $^{48}\text{Ca}$  to  $^{70}\text{Zn}$  [1]. Clearly, comparing with Pb/Bi based reactions, the entrance channel is more symmetric and there are no closed shells, the cross sections will be then reduced. But on the other hand, the accessible compound nuclei are richer by 2 neutrons (except for element 111) and this will be in favour of the cross sections.

An estimation of the reduction factors (see Figure 3) can be made using the compound nucleus  $^{220}\text{Th}$  produced via different entrance channels having similar Bass barriers [4, 10, 11, 12]:  $\text{Ar}_{18}+\text{Hf}_{72}$  and  $\text{Zn}_{30}+\text{Nd}_{60}$  systems have no closed shells and the more symmetric system has a cross section smaller by a factor 14. Assuming a steady variation with the charge asymmetry, the expected cross sections for  $\text{Ca}_{20}+\text{Yt}_{70}$  and  $\text{Zr}_{40}+\text{Sn}_{50}$  are estimated. The actual cross sections are much higher, by a factor 6 and 23 respectively, due to the role of the closed shells [13]. These factors may now be used to estimate the reduction factor which applies when the same CN is formed on  $^{76}\text{Ge}$  based reactions in comparison with Pb/Bi based reactions. The loss of shell effects is estimated to reduce the cross section by one order of magnitude (represented by a solid arrow in Figure 3). At  $Z=106$ , the decrease of asymmetry reduces the cross section by a factor about 12 (represented

by a dashed arrow in Figure 3) whereas this asymmetry disappears for  $^{76}\text{Ge}+^{208}\text{Pb}$  reaction producing element 114.

An estimation of the gain in the cross section due to the neutron richness can be made also considering the Th isotopes. Detailed measurements show that 2 more neutrons in the CN increase the residue cross section by a factor 9 [12]. As seen in Figure 3, the gain for Z=110 using  $^{64}\text{Ni}$  beam instead of  $^{62}\text{Ni}$  is in the order of 5. In our estimation for  $^{76}\text{Ge}$  beam, we consider an average factor of 7 (represented by a solid arrow on Figure 3). Then, the estimated cross sections are represented by solid crosses. They are smaller than the Pb/Bi based cross sections.

### 4.3 Study of the structure of the Super Heavy Elements

A new experimental program is proposed at GANIL [14] on the study of transfermium isotopes by the use of spectroscopic information in order to have a better understanding of their shell structure. This program is going to start with the  $\alpha$ ,  $\gamma$  and electron spectroscopy of  $^{251}\text{Md}$  and  $^{251}\text{Fm}$ .  $^{251}\text{Md}$  is populated by the  $\alpha$ -decay of  $^{255}\text{Lr}$  produced in the 2 neutrons channel of the  $^{48}\text{Ca}+^{209}\text{Bi}$  fusion evaporation reaction. The  $^{251}\text{Md}$  should decay with less than 10% by  $\alpha$ -decay on  $^{247}\text{Es}$  and with more than 90% by EC on  $^{251}\text{Fm}$ . Since the ground state parity and spin of the first level of  $^{251}\text{Fm}$  are known, ground state of  $^{251}\text{Fm}$  and possibly of  $^{255}\text{Lr}$  could be determined. The experimental setup will be adapted with a tunnel of Si detectors to detect conversion-electrons and a set of Ge clover detectors from Exogam will be added in a close geometry.

## Acknowledgements

The authors would like to acknowledge all the technicians and engineers from mechanics, detector and electronic groups who made possible this experimental program, especially at LPC Caen, GANIL and Saclay. We are also indebted to the target laboratories of LNS Catania, IFU Sao Paulo, GSI Darmstadt and IPN Orsay for the excellent quality of their products. The users support group (Service des aires) and the accelerator staff of GANIL should be mentioned for their continuous support and efficient performances at all stages of this work. Finally, a great help was provided by the data acquisition group GIP (GANIL) for the electronics and by the CHARISSA collaboration for lending us their VXI ADC's.

## References

- [1] S. Hofmann and G. Münzenberg, *Rev. Mod. Phys.***72**(2000)733.
- [2] R. Anne and A. C. Mueller, *NIM B***70**(1992)276.
- [3] Simulation code ZGOUBY, F. Méot and S. Valéro, SATURNE Note LNS/GT/93-12
- [4] C. C. Sahm *et al.*, *Nucl. Phys A***441**(1985)316.
- [5] V. Ninov *et al.*, *Phys. Rev. Lett.***83**(1999)104.
- [6] V. Ninov *et al.*, submitted to *Phys. Rev. Lett.* (August 2001).
- [7] S. Hofmann, *Proc. Int. Conf. Sevilla 1999*.

- [8] J. Péter *et al.*, proposal for GANIL experiment E339b(09-2000).
- [9] C. Stodel *et al.*, proposal for GANIL experiment E369a(09-2000).
- [10] C. C. Sahm *et al.*, *Z. Phys A***319**(1984)113.
- [11] D. Vermeulin *et al.*, *Z. Phys A***318**(1984)157.
- [12] C. Stodel, PhD thesis, LPC Caen, LPC-C T98-05 (1998), unpublished.
- [13] P. Möller *et al.*, *Z. Phys A***359**(1997)251.
- [14] C. Theisen *et al.*, proposal for GANIL experiment E375(2000).



Table I: Summary of the different possible reactions using  $^{207,208}\text{Pb}$  beams on various targets.  $Z_{CN}$  and  $A_{CN}$  are respectively the atomic number and mass of the compound nucleus,  $E_{bass}^*$  being the excitation energy at the Bass barrier.

$Z_{CN}$	$^{208}\text{Pb}$ beam			$^{207}\text{Pb}$ beam		
	Target	$A_{CN}$	$E_{bass}^*$ (MeV)	Target	$A_{CN}$	$E_{bass}^*$ (MeV)
104	$^{50}\text{Ti}$	258	23	$^{50}\text{Ti}$	257	23
105	$^{51}\text{V}^a$	259	25	$^{51}\text{V}$	258	25
106	$^{54}\text{Cr}$	262	22	$^{54}\text{Cr}$	262	22
107	$^{55}\text{Mn}^a$	263	24	$^{55}\text{Mn}^b$	262	24
108	$^{58}\text{Fe}$	266	21	$^{58}\text{Fe}$	265	20
109	$^{59}\text{Co}^a$	267	23	$^{59}\text{Co}^b$	266	22
110	$^{64}\text{Ni}$	272	17	$^{64}\text{Ni}$	271	16
111	$^{65}\text{Cu}^a$	273	19	$^{65}\text{Cu}^b$	272	18
112	$^{70}\text{Zn}$	278	12	$^{70}\text{Zn}^b$	277	12
113	$^{71}\text{Ga}$	279	13	$^{71}\text{Ga}$	278	13
114	$^{76}\text{Ge}$	284	9	$^{76}\text{Ge}$	283	9
115	$^{75}\text{As}$	283	13	$^{75}\text{As}$	282	13
116	$^{82}\text{Se}$	290	3	$^{82}\text{Se}$	289	2
117	$^{81}\text{Br}$	289	7	$^{81}\text{Br}$	288	6

new reactions, <sup>a</sup> new path, <sup>b</sup> production of new isotope

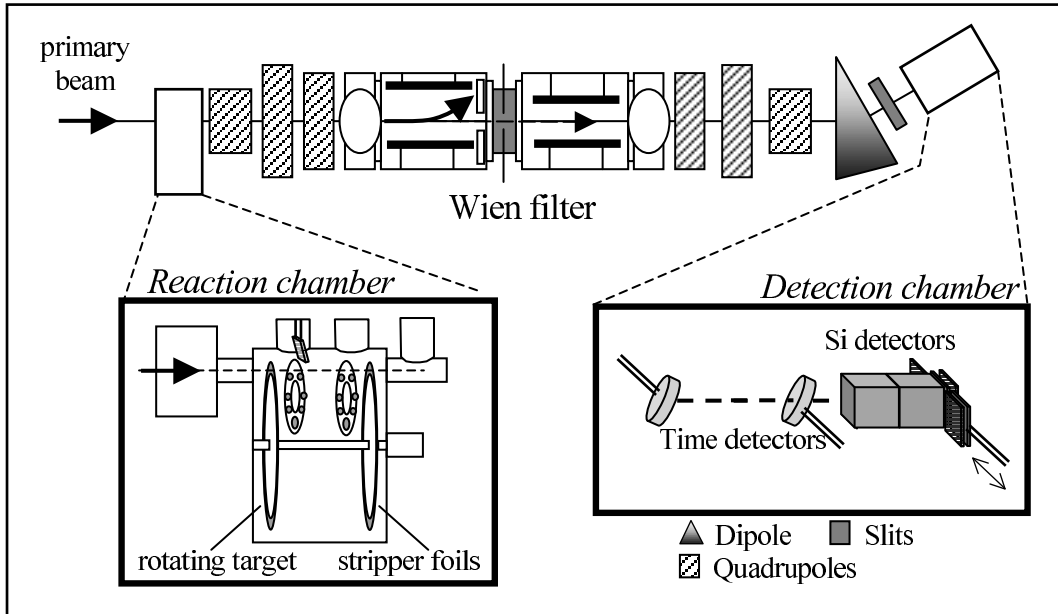


Figure 1: Schematic drawing of the experimental setup including, from left to right, the reaction chamber with the rotating target and stripper foils, the Q-poles and the LISE3 Wien filter between them, the last dipole and the detection chamber with time and Si detectors.

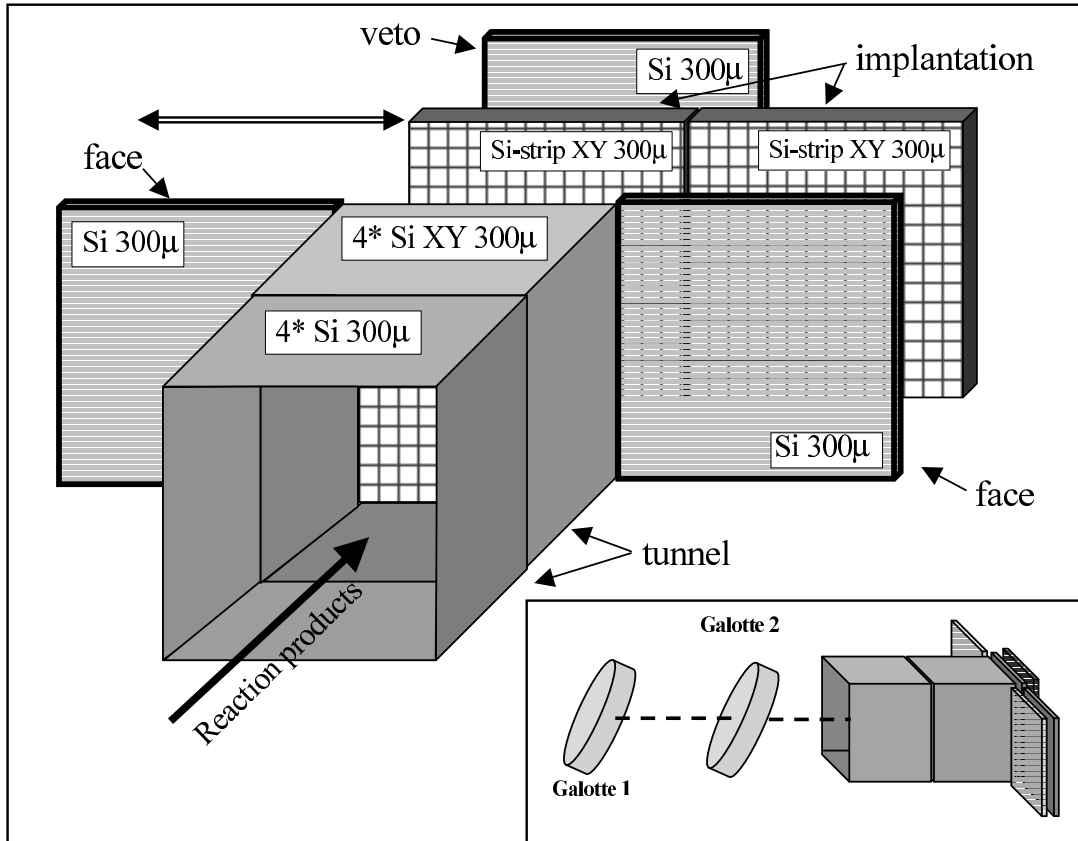


Figure 2: Schematic view of the detection setup implanted at the end of the LISE3 spectrometer. It is composed by 2 time detectors (Galotte), 2 movable implantation Si detectors, a set of 8 Si detectors for the tunnel, 1 veto Si detector behind the 'in beam' implantation and 2 Si detectors (face) to recover the products ( $\alpha$  or fission fragment) escaping the 'out of beam' implantation detector.

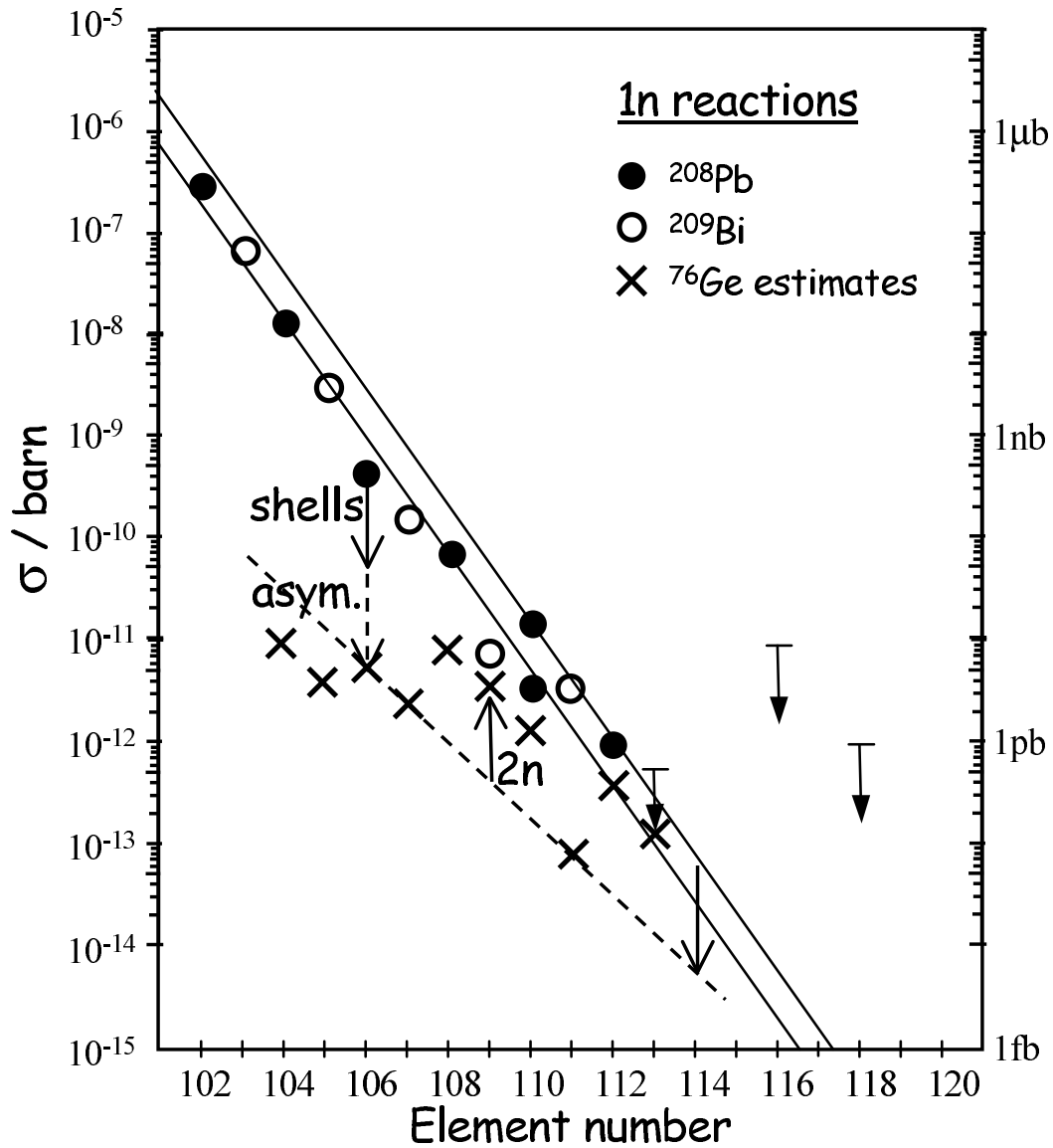


Figure 3: One neutron channel cross sections measured for  $^{208}\text{Pb}$  and  $^{209}\text{Bi}$  targets in direct kinematics [7]. The crosses represent our estimations using a  $^{76}\text{Ge}$  beam (see text sect. 4.2. for details).